



TOTAL CROSS SECTIONS OF P AND  $\bar{P}$   
ON PROTONS AND DEUTERONS BETWEEN 50 AND 200 GeV/c

A. S. Carroll, I-H. Chiang, T. F. Kycia, K. K. Li, P. O. Mazur,  
P. Mockett, D. C. Rahm, and R. Rubinstein  
Brookhaven National Laboratory, Upton, New York 11973

and

W. F. Baker, D. P. Eartly, G. Giacomelli,  
P. F. M. Koehler, K. P. Pretzl, and A. A. Wehmann  
Fermi National Accelerator Laboratory, Batavia, Illinois 60510

and

R. L. Cool and O. Fackler  
Rockefeller University, New York, New York 10021

July 1974



TOTAL CROSS SECTIONS OF P AND  $\bar{P}$  ON  
PROTONS AND DEUTERONS BETWEEN 50 AND 200 GeV/c\*

A. S. Carroll, I-H. Chiang, T. F. Kycia, K. K. Li, P. O. Mazur,  
P. Mockett<sup>§</sup>, D. C. Rahm, R. Rubinstein<sup>†</sup>

Brookhaven National Laboratory, Upton, New York 11973

and

W. F. Baker, D. P. Eartly, G. Giacomelli,<sup>†</sup>  
P. F. M. Koehler, K. P. Pretzl,<sup>+</sup> and A. A. Wehmann

Fermi National Accelerator Laboratory

P. O. Box 500, Batavia, Illinois 60510

and

R. L. Cool, and O. Fackler

Rockefeller University, New York, New York 10021

ABSTRACT

Proton and antiproton total cross sections on protons and deuterons have been measured at 50, 100, 150 and 200 GeV/c. The proton cross sections rise with increasing momentum. Antiproton cross sections fall with increasing momentum, but the rate of fall decreases between 50 and 150 GeV/c, and from 150 to 200 GeV/c there is little change in cross section.

We have measured  $p$  and  $\bar{p}$  total cross sections on protons and deuterons in 50 GeV/c steps between 50 and 200 GeV/c. The experiment, which was carried out in the M1 beam<sup>1,2</sup> at the Fermi National Accelerator Laboratory, used a "good geometry" transmission technique.

Incident particles were defined by scintillation counters and identified by two differential gas Cerenkov counters<sup>3</sup>, allowing cross sections of two different particles to be measured simultaneously; in addition, a threshold gas Cerenkov counter<sup>4</sup> could be used in anticoincidence when required. Contamination of unwanted particles in the selected  $p$  and  $\bar{p}$  beams was always below 0.1%.

The 3 meter long liquid hydrogen and deuterium targets and an identical evacuated target were surrounded by a common outer jacket of liquid hydrogen for temperature stability<sup>5</sup>. By continuously monitoring the vapor pressure in the outer jacket, the target temperature, and therefore the hydrogen and deuterium densities were determined<sup>6</sup>; density variations were less than .07% throughout the experiment. For each run a weighted average of the density for that run was used. Target lengths were measured under operating conditions to  $\pm .03\%$ .

The transmission through the targets was measured by 12 scintillation counters of different diameters, with 11 independent channels being formed by coincidences between pairs of adjacent counters to minimize accidental counts and

tube noise. These counters were mounted together, smallest upstream, on a moveable cart and were positioned such that for each momentum the counters accepted the same range of  $|t|$ , extending up to  $0.008 \text{ (GeV/c)}^2$  for the smallest channel and up to  $0.08 \text{ (GeV/c)}^2$  for the largest. The efficiencies of the transmission counters were measured at frequent intervals throughout the experiment using two small counters placed behind them. Such efficiencies were constant and always  $> 99.8\%$

For each momentum, the beam was tuned to give a final focus at the transmission counters. Two sets of proportional wire chambers were in the incident beam, each set giving two coordinates, and a matrix coincidence was set up between appropriate wires to ensure that each incident particle trajectory would pass through a 2 cm square at the transmission counters<sup>7</sup>. This technique eliminates systematic effects in the extrapolation procedure from beam halo and possible beam instability. In addition, the electronic logic for these chambers required that one and only one particle register in each chamber. This, together with large veto counters around the beam, eliminated possible fluctuations due to accidentals. Cross sections were found to be stable to better than 0.2% for variations in beam flux of a factor of 3 around the value ( $2 \times 10^5$  per pulse) at which data were normally taken. Proportional chambers on the transmission counter cart were used to check that the beam was correctly positioned and focussed before data taking commenced.

The experiment was monitored on-line by a PDP-15 computer. The three targets were interchanged remotely at least once an hour, and a minimum of four cycles of the targets were taken at each momentum.

The data were corrected<sup>8</sup> for single coulomb scattering (< 0.1%) and coulomb-nuclear interference (< 0.3%). For the latter, the ratio  $\rho$  of real to imaginary parts of the forward scattering amplitude was obtained from Bartenev et al.<sup>9</sup> for pp and the predictions of Cheng et al.<sup>10</sup> for  $\bar{p}p$ . The value of  $\rho$  for neutrons was assumed to be the same as for protons. A correction to the data was applied for the 0.65% measured HD contamination in the liquid deuterium.

The extrapolation to  $t = 0$  of the partial cross sections was carried out using the expression

$$\sigma_i = \sigma_T \exp \{At_i + Bt_i^2 + Ct_i^3\}$$

where  $\sigma_i$  is the partial cross section measured by the  $i^{\text{th}}$  transmission counter combination subtending a maximum  $|t_i|$ , and  $\sigma_T$  is the total cross section. For all of the four cross sections measured here, the  $Bt_i^2$  term was necessary, as determined by a substantial reduction in the  $\chi^2$  of the fit when it was added. For cross sections on protons, there was no change in the total cross section when the  $Ct_i^3$  term was added, nor was there any change in  $\chi^2$ , and so C was set equal to zero; for deuteron cross sections, the  $Ct_i^3$  term was found to substantially improve the fit. The extrapolations were carried out using the 3rd through 10th transmission

counter combinations, covering  $0.012 \leq |t_i| \leq 0.062 \text{ (GeV/c)}^2$ . Using fewer counters changed the results by less than 0.1%, indicating negligible multiple coulomb scattering and beam size effects in the counters used for the extrapolation. This method, of course, cannot take into account a rapid change in slope below  $0.012 \text{ (GeV/c)}^2$ .

From the reproducibility of our data we quote a momentum dependent uncertainty in the results for a particular incident particle of  $\pm 0.15\%$  for those cross sections where the statistical error was smaller than this. The momentum independent scale uncertainty for the absolute magnitude of the cross section, caused by uncertainties in the form of the extrapolation and in the hydrogen and deuterium densities and contaminations, is estimated to be  $\pm 0.5\%$  for protons and  $\pm 0.6\%$  for deuterons.

The results are listed in Table I and shown in Figures 1 and 2, together with previous data<sup>11-21</sup>. Agreement with other experiments in the same momentum range is within the quoted scale errors, except for that of Gustafson et al.<sup>21</sup>

As the incident momentum increases from 50 to 200 GeV/c the pp total cross section rises by 2%. The rise is consistent with the rise observed at the CERN ISR<sup>17,18</sup>. The  $\bar{p}p$  cross sections continue to fall with increasing momentum, but the rate decreases markedly, and above 150 GeV/c there is very little variation.

Cross sections of p and  $\bar{p}$  on deuterons show a momentum

dependence similar to those on protons. The  $\bar{p}d$  cross section is also nearly constant above 150 GeV/c.

The antiparticle-particle differences  $\sigma_{\bar{p}p} - \sigma_{pp}$  and  $\sigma_{\bar{p}d} - \sigma_{pd}$  are shown in Fig. 3. These differences are becoming smaller with increasing momentum, and can be fitted by the form  $As^{\alpha-1}$ . Using only data from this experiment gives  $\alpha = 0.39 \pm 0.04$  for  $\sigma_{\bar{p}p} - \sigma_{pp}$  and  $\alpha = 0.43 \pm 0.05$  for  $\sigma_{\bar{p}d} - \sigma_{pd}$ . If this form for  $\sigma_{\bar{p}p} - \sigma_{pp}$  is extrapolated to higher momentum, together with the known  $\sigma_{pp}$ , an estimate of  $\sigma_{\bar{p}p}$  at higher momenta can be obtained. This procedure predicts a minimum in the antiproton-proton cross section at about 200 GeV/c.

The purpose of measuring deuteron cross sections is to extract cross sections on neutrons. We have done this to within the accuracy of the Glauber-Wilkin formula<sup>22, 23</sup>, which takes into account the shadowing in the deuteron. A parameter  $\langle r^{-2} \rangle$  is used in the formula, and we have derived it from our pion data<sup>24</sup>; it is consistent with being momentum independent and averages  $0.039 \text{ mb}^{-1}$ . There has been recent discussion as to whether this parameter is dependent upon the incident particle, or whether a more complex formula should be used<sup>25-28</sup>. Using the work of Gorin et al.<sup>28</sup> our measured value of  $\langle r^{-2} \rangle$  would be scaled to  $0.031 \text{ mb}^{-1}$  for incident protons. In view of the uncertainties in the method, we have used a value of  $0.035 \text{ mb}^{-1}$  with a systematic uncertainty of  $\pm 0.004 \text{ mb}^{-1}$  in extracting pn and  $\bar{p}n$  cross sections. We note that this systematic uncertainty causes a  $\pm 1.5\%$  scale uncertainty

in the neutron cross sections, but does not affect the momentum dependence. We note further that the cross sections on neutrons shown in Fig. 1b have a behavior with momentum similar to those on protons. The difference  $\sigma_{\bar{p}n} - \sigma_{pn}$ , which is only slightly affected by the value of  $\langle r^{-2} \rangle$ , is shown in Fig. 3, and also shows the same behavior as on protons.

We have applied the method of Bronzan et al.,<sup>29</sup> to derive the real parts of forward scattering amplitudes. For protons, we find a real part in agreement with the results of Bartenev et al.,<sup>9</sup> while for  $\bar{p}p$  the prediction is for the real part to pass through zero near 80 GeV/c.

REFERENCES

- \* Work supported by the U. S. Atomic Energy Commission.
- <sup>5</sup> Present address: Physics Department, University of  
Washington, Seattle, Washington 98195
- <sup>‡</sup> Present address: Fermi National Accelerator Laboratory  
P. O. Box 500, Batavia, Illinois 60510
- <sup>†</sup> Visitor from Istituto di Fisica. University of Padova,  
and INFN, Sezione di Padova, Padova, Italy.
- <sup>+</sup> Present address: Max Planck Institute for Physics and  
Astrophysics, Munich, Germany
- <sup>1</sup> Meson Laboratory Preliminary Design Report. J. R. Orr  
and A. L. Read, NAL (1971) (Unpublished).
- <sup>2</sup> W. F. Baker, et al., NAL Report, NAL-Pub.-74/13-EXP and to  
be published.
- <sup>3</sup> T. F. Kycia - to be published.
- <sup>4</sup> S. M. Pruss, NAL Report TM-470 and to be published.
- <sup>5</sup> Targets of similar construction have been described in  
References 8 and 11.
- <sup>6</sup> R. J. Tapper, Rutherford Laboratory Report NIRL/R/95 (1965).
- <sup>7</sup> A. S. Carroll, et al., to be published.
- <sup>8</sup> R. L. Cool, et al., Phys. Rev. D1, 1887, (1970).
- <sup>9</sup> V. Bartenev, et al., Phys. Rev. Letters 31, 1367 (1973).
- <sup>10</sup> H. Cheng, et al., Phys. Letters 44B, 283, (1973).
- <sup>11</sup> W. Galbraith, et al., Phys. Rev. 138, B913, (1965).
- <sup>12</sup> K. J. Foley, et al., Phys. Rev. Letters 19, 857, (1967).
- <sup>13</sup> S. P. Denisov, et al., Phys. Letters 36B, 415, (1971).
- <sup>14</sup> S. P. Denisov, et al., Phys. Letters 36B, 528, (1971).

- <sup>15</sup>S. P. Denisov, et al., Nucl. Phys. B65, 1, (1973).
- <sup>16</sup>C. Bromberg, et al., Phys. Rev. Letters 31, 1563, (1973).
- <sup>17</sup>U. Amaldi, et al., Phys. Letters 44B, 112, (1973).
- <sup>18</sup>S. R. Amendolia, et al., Phys. Letters 44B, 119 (1973).
- <sup>19</sup>G. Charlton, et al., Phys. Rev. Letters 29, 515 (1972).
- <sup>20</sup>F. T. Dao, et al., Phys. Rev. Letters 29, 1627, (1972).
- <sup>21</sup>H. R. Gustafson, et al., Phys. Rev. Letters 32, 441, (1974).
- <sup>22</sup>R. J. Glauber, Phys. Rev. 100, 242, (1955).
- <sup>23</sup>C. Wilkin, Phys. Rev. Letters 17, 561 (1966).
- <sup>24</sup>A. S. Carroll, et al., following paper.
- <sup>25</sup>J. Pumplin and M. Ross, Phys. Rev. Letters 21, 1778, (1968).
- <sup>26</sup>V. V. Anisovich, et al., Phys. Letters 42B, 224, (1972).
- <sup>27</sup>D. Sidhu and C. Quigg, Phys. Rev. D7, 755, (1973)., C. Quigg  
and L. L. Wang, Phys. Letters 43B, 314 (1973).
- <sup>28</sup>Yu. P. Gorin, et al., Sov. Journ. Nucl. Phys. 15, 530, (1972)  
(Yad Fiz 15, 953 (1972)).
- <sup>29</sup>J. B. Bronzan, et al., Phys. Letters 49B, 272, (1974).

TABLE I  
RESULTS OF THIS EXPERIMENT. CROSS SECTIONS IN MILLIBARNS

	MOMENTUM (Gev/c)				Momentum independent scale uncertainty
	50	100	150	200	
$\sigma_{pp}$	38.14±0.07	38.39±0.06	38.62±0.06	38.90±0.06	±0.5%
$\sigma_{pd}$	72.98±0.13	73.12±0.11	73.46±0.11	73.84±0.11	±0.6%
$\sigma_{\bar{p}p}$	43.86±0.11	42.04±0.09	41.72±0.18	41.54±0.29	±0.5%
$\sigma_{\bar{p}d}$	82.21±0.24	79.32±0.19	78.24±0.35	78.77±0.57	±0.6%
$\sigma_{pn}$	38.86±0.16	38.85±0.14	39.02±0.14	39.18±0.14	±1.5%
$\sigma_{\bar{p}n}$	43.69±0.30	42.22±0.23	41.32±0.44	42.09±0.71	±1.5%
$\sigma_{\bar{p}p} - \sigma_{pp}$	5.72±0.13	3.65±0.11	3.10±0.19	2.64±0.30	
$\sigma_{\bar{p}d} - \sigma_{pd}$	9.23±0.28	6.20±0.22	4.78±0.37	4.92±0.58	
$\sigma_{\bar{p}n} - \sigma_{pn}$	4.83±0.34	3.37±0.27	2.30±0.46	2.91±0.72	

FIGURE CAPTIONS

Figure 1: Total cross sections for  $pp$  and  $\bar{p}p$ . Momentum dependent errors only are shown. Data of other experiments are from References 11 - 21.

Figure 2: Total cross sections for  
a)  $pd$  and  $\bar{p}d$ ,  
b)  $pn$  and  $\bar{p}n$ .  
Momentum dependent errors only are shown.  
References as for Figure 1.

Figure 3: Values of total cross section differences  
 $\sigma_{\bar{p}d} - \sigma_{pd}$ ,  $\sigma_{\bar{p}p} - \sigma_{pp}$  and  $\sigma_{\bar{p}n} - \sigma_{pn}$ .  
References as for Fig. 1.

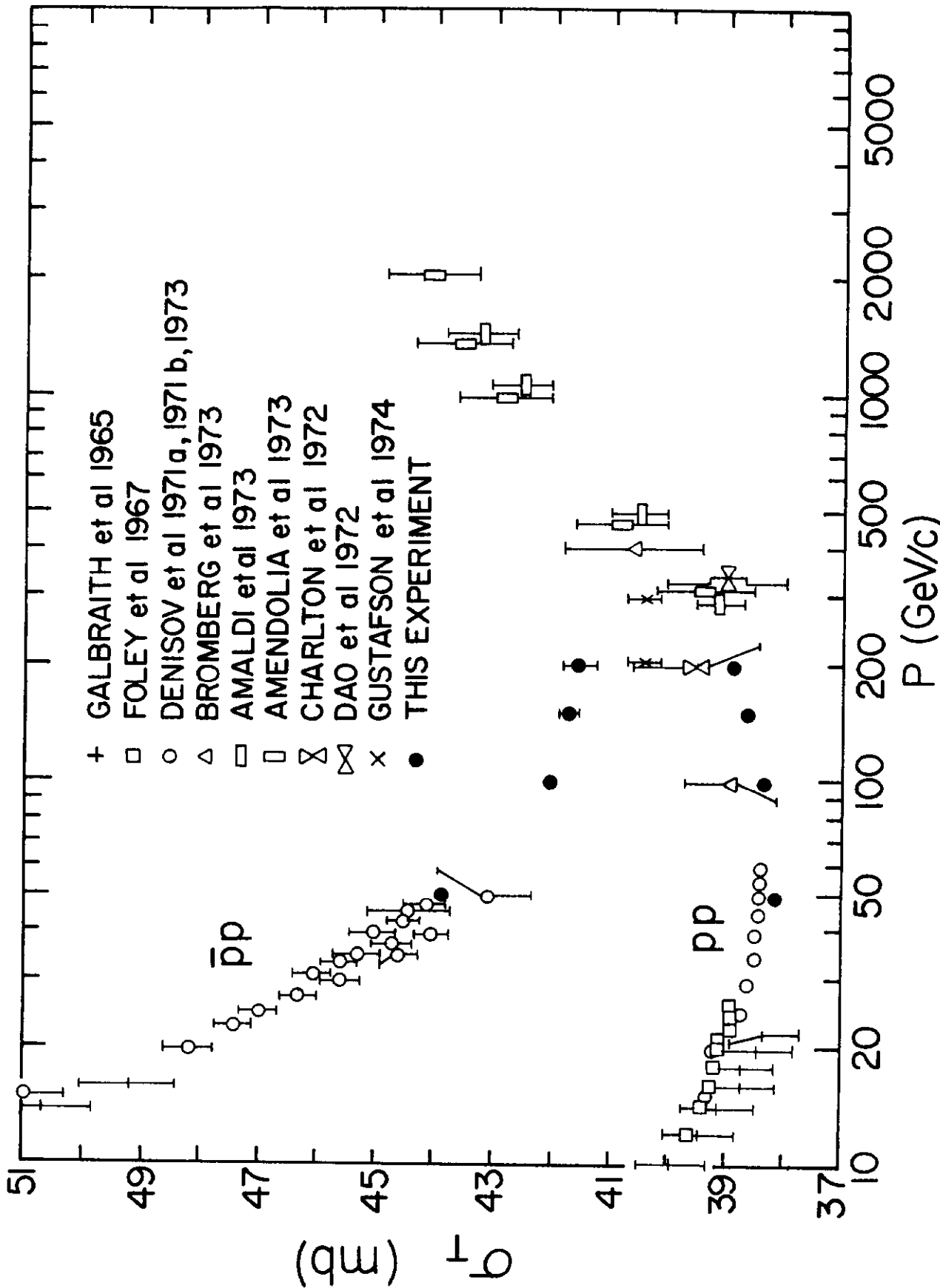


Fig. 1

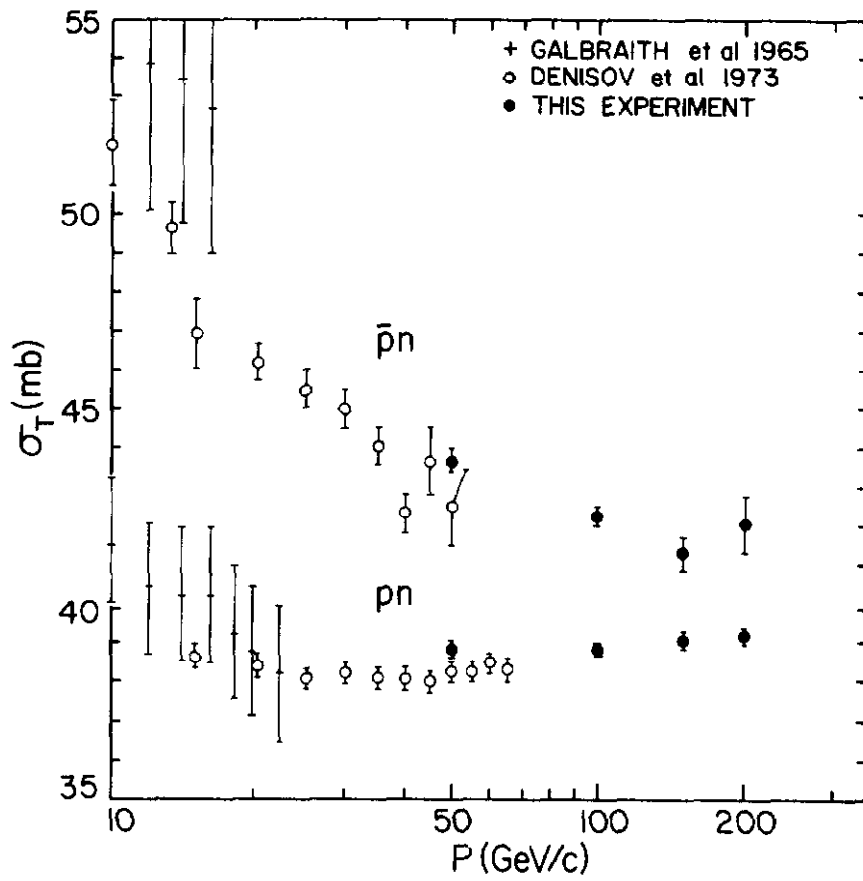
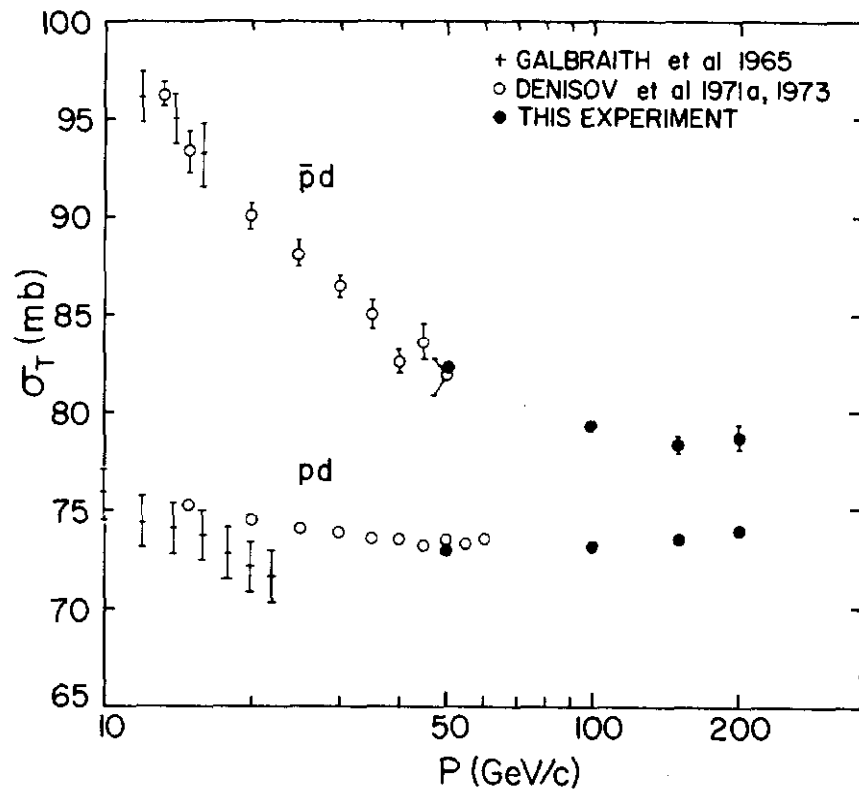


Fig. 2

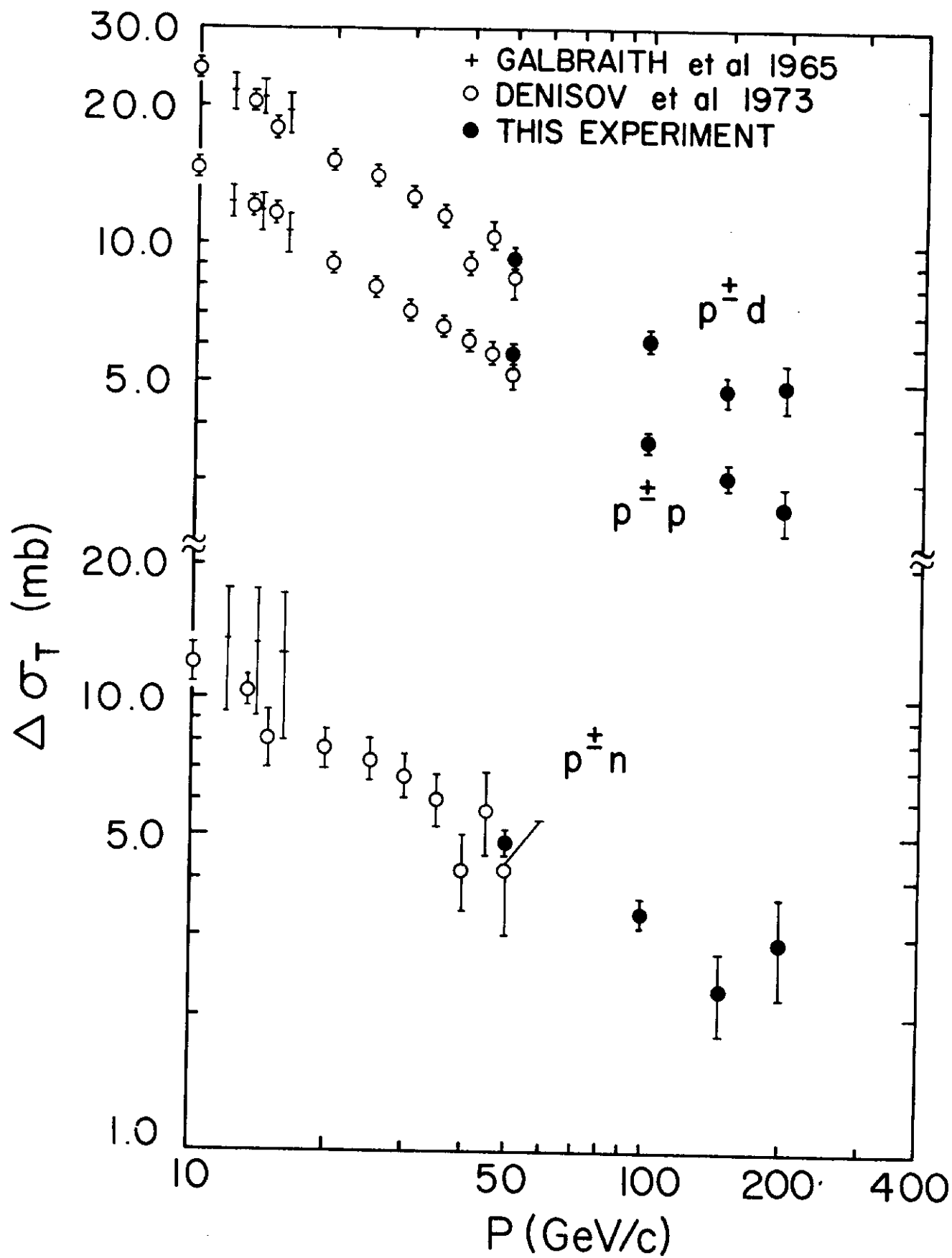


Fig. 3